

ELICIT AND ENHANCE: ADVANCING MULTIMODAL REASONING IN MEDICAL SCENARIOS

000
001
002
003
004
005 **Anonymous authors**
006 Paper under double-blind review
007
008
009
010

ABSTRACT

011 Effective clinical decision-making depends on iterative, multimodal reasoning
012 across diverse sources of evidence. The recent emergence of multimodal reasoning
013 models has significantly transformed the landscape of solving complex tasks.
014 Although such models have achieved notable success in mathematics and science,
015 their application to medical domains remains underexplored. In this work, we
016 propose *MedE*², a two-stage post-training pipeline that elicits and then enhances
017 multimodal reasoning for medical domains. In Stage-I, we fine-tune models using a
018 limited number of text-only data samples containing precisely orchestrated reasoning
019 demonstrations to elicit reasoning behaviors. In Stage-II, we further enhance
020 the model’s reasoning quality using rigorously curated multimodal medical cases,
021 aligning model reasoning outputs with our proposed multimodal medical reasoning
022 preference. Extensive experiments demonstrate the efficacy and reliability of
023 *MedE*² in improving the reasoning performance of medical multimodal models.
024 Notably, models trained with *MedE*² consistently outperform baselines across
025 multiple medical multimodal benchmarks. Additional validation on larger models
026 and under inference-time scaling further confirms the robustness and practical
027 utility of our approach.
028

1 INTRODUCTION

029
030 Medicine is a multifaceted endeavor. It requires clinicians to process vast amounts of information,
031 including patient medical histories, physical examination findings, and laboratory test results, to
032 diagnose conditions, formulate prognoses, and determine appropriate treatment plans. In many
033 clinical settings, an iterative reasoning process that evaluates multiple possibilities with progressively
034 accumulated clinical information is considered fundamental to medical practice (Adler-Milstein et al.,
035 2021; Singh et al., 2022; Croskerry & Clancy, 2022). Recent advancements in multimodal large
036 language models (MLLMs), such as OpenAI-o-series (OpenAI, 2024) and Gemini-2.5-Pro (Google,
037 2025), have significantly advanced complex task performance. These models employ scaling inference
038 time and emulate reflective cognitive processes, pushing capabilities to unprecedented levels. In
039 light of these advancements, we explore the question: *How can we effectively extend the strategy of*
040 *multimodal reasoning to medical domains?*

041 We begin by evaluating the capabilities of different models within the medical domain, as such
042 assessments provide a natural starting point for probing a model’s medical knowledge and reasoning
043 abilities. The results shown in the left panel of Figure 1 indicate that current multimodal models (i.e.,
044 general-purpose (Bai et al., 2025b; Chen et al., 2024b) and those specifically designed for medical
045 tasks (Chen et al., 2024a; Li et al., 2023)) demonstrate strong performance on relatively simple
046 visual question answering tasks (Liu et al., 2021; Lau et al., 2018). However, performance declines
047 markedly on more complex tasks (Yue et al., 2024a;b), which require deeper comprehension and
048 advanced reasoning. Since effective reasoning models should be grounded in robust foundation
049 models (Ye et al., 2025), we adopt general-purpose MLLMs as the basis for developing specialized
050 medical reasoning models.

051 Previous research (DeepSeek-AI, 2025; Ye et al., 2025; Li et al., 2025) primarily relied on carefully
052 curated, challenging datasets from mathematical and scientific domains to incentivize the model’s
053 reasoning capacity. In contrast, although medical practice encompasses numerous scenarios requiring
reasoning, the available data remain limited, especially those integrating clinical information. To

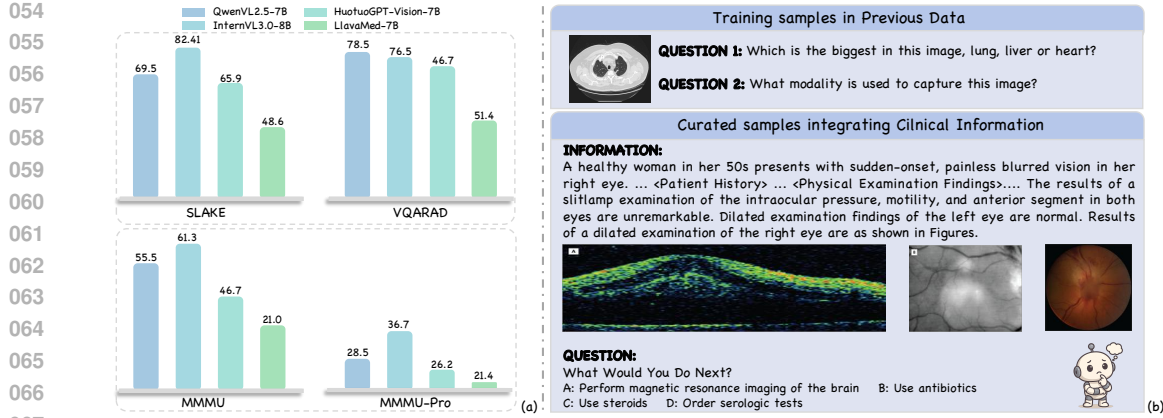


Figure 1: (a) Current models’ performance on diverse tasks. (b) Samples that closely mirror real-world clinical scenarios are used to strengthen multimodal reasoning capabilities instead of samples focused primarily on pattern recognition or basic knowledge recall.

alleviate this, we adopt a rigorous data construction process involving meticulous data collection, cleaning, and expert review. Unlike earlier studies (Pan et al., 2025; Lai et al., 2025) that relied primarily on simple question–answer pairs solvable through memorized knowledge or pattern recognition (Figure 1), our curated dataset comprises 3K textual questions and 2K multimodal questions spanning 12 imaging modalities, including radiology, pathology, and optical coherence tomography. These samples are sourced from authoritative examinations (Jin et al., 2021) and publicly available case reports published in leading medical journals (PubMed, 2003). Each multimodal case integrates clinical histories, physical examinations, diagnostic investigations, and procedures.

With the dataset in place, we proceed to develop the models’ reasoning capabilities specifically for clinical scenarios. Most of current work (Meng et al., 2025; DeepSeek-AI, 2025; Su et al., 2025; Li et al., 2025) usually employs rule-based reinforcement learning (Shao et al., 2024) to advance models’ reasoning capabilities. However, challenges such as normalization of specialized medical terms (e.g., anatomical terminology) and hierarchical relationships (e.g., organ-system classifications) in medical domains make it difficult to verify responses solely through predefined rules. Moreover, the prevalent strategy that relies on outcome-based rewards is vulnerable to hallucinations during the reasoning process. This poses significant risks in clinical applications, where diagnostic and therapeutic decision-making demands exceptional logical rigor and strong evidence-based justification. Building upon these, we introduce a novel training pipeline, named *MedE*². Our pipeline involves two stages to progressively elicit and enhance the clinical cognitive reasoning capability of the models. Instead of *cold-start* on multimodal data (DeepSeek-AI, 2025), in the first stage, we conduct supervised fine-tuning on text-only data, where each sample includes carefully designed reasoning demonstrations to show how to utilize existing knowledge to solve complex tasks. Subsequently, we enhance the quality of the generated reasoning process to align with desired patterns. During this stage, we formulate Multimodal Medical Reasoning Preference (MMRP) and utilize Gemini-2.5-Pro to perform rejection sampling on our curated dataset, while employing Direct Preference Optimization (DPO) (Ziegler et al., 2019; Ouyang et al., 2022) to calibrate and refine the model’s capabilities.

Extensive experiments are conducted to validate the effectiveness of our proposed pipeline. Despite being trained only on text-based reasoning data during Stage-I, the models demonstrate significant performance improvements across multiple medical benchmarks, achieving gains of at least 4.45% on MedXpertQA-MM (Zuo et al., 2025) and 6.67% on MMMU-Pro-Health (Yue et al., 2024b). These results highlight an innovative method for eliciting reasoning behaviors in multimodal medical tasks. Further enhancement in Stage-II enables models to exhibit superior reasoning capabilities, reaching performance competitive with several larger-scale models. We also show that improvements from *MedE*² generalize well to models with larger parameters. Moreover, the consistent improvements observed under inference-time scaling further demonstrate the robustness of our post-training recipe. In summary, our main contributions are as follows:

- 108 • We present *MedE*², a two-stage post-training pipeline to enhance multimodal reasoning in
109 medical scenarios: (1) eliciting reasoning behavior by leveraging strategically developed
110 text-only datasets, and (2) refining the reasoning quality by incorporating meticulously
111 curated multimodal data.
- 112 • We construct a high-quality dataset of approximately 5,000 samples, comprising both
113 text-based questions with reasoning chains and multimodal questions involving clinical
114 information, thereby establishing a reliable corpus for bootstrapping medical reasoning.
- 115 • We perform comprehensive experiments across diverse benchmarks. Experimental results
116 consistently demonstrate that *MedE*² significantly enhances model performance and achieves
117 strong generalization across models of varying sizes, while also being robust to inference-
118 time scaling.

120 2 RELATED WORK

121 2.1 MEDICAL MULTIMODAL LARGE LANGUAGE MODELS

124 The development of multimodal large language models has significantly advanced the field of
125 medicine. Current medical multimodal large language models are primarily based on general
126 multimodal models and are further trained on specialized medical datasets. This approach led
127 to the emergence of numerous medical multimodal large models. For example, Med-PaLM (Tu
128 et al., 2024) constructs the MultiMedBench dataset and fine-tunes based on PaLM-E (Driess et al.,
129 2023). Recent studies continuously use similar strategies and refined training methods, resulting
130 in significant progress, such as LLaVA-Med (Li et al., 2023), BioMedGPT (Zhang et al., 2024),
131 MedTrinity-25M (Xie et al., 2024), and Med-Gemini (Saab et al., 2024). These strategies have
132 demonstrated good application results in various medical scenarios, including medical dialogue (Ye
133 et al., 2023), clinical decision support (Schubert et al., 2023), electronic health record analysis (Luo
134 et al., 2022), and image report generation (Li et al., 2018). As an endeavor that involves multi-level
135 analysis of details, the reasoning ability is vital for solving medical tasks. In this study, we aim to
136 explore how to incentivize the reasoning abilities of multimodal large models in medical tasks.

137 2.2 REASONING MODELS

139 Enhancing the reasoning abilities of models remains a key challenge. Early efforts evolved from
140 few-shot prompting to structured paradigms like Chain-of-Thought (Wei et al., 2022) and ReAct (Yao
141 et al., 2023), aiming to emulate human-like reasoning. Subsequent work recognized reasoning as an
142 iterative trial, error, and refinement process. The release of OpenAI’s o1 (OpenAI, 2024) catalyzed
143 further progress. Journey Learning (Qin et al., 2024) explored strategies for o1-style slow thinking
144 and STILL-2 (Min et al., 2024) distilled long-form reasoning data to expand and refine solution
145 paths. These advancements, culminating in DeepSeek’s results (DeepSeek-AI, 2025), highlight the
146 critical role of reinforcement learning in improving reasoning. Diverse reinforcement learning (RL)
147 approaches to further bolster reasoning are now being actively explored and investigated (Wang et al.,
148 2024; Wei et al., 2025). However, effective training strategies to enhance the reasoning abilities of
149 medical models are still lacking. Previous research has primarily focused on constructing reasoning
150 processes or adapting reinforcement learning (RL) frameworks (Su et al., 2025; Sun et al., 2025; Pan
151 et al., 2025; Lai et al., 2025). In this paper, we propose a novel two-stage post-training recipe that
152 progressively elevates models’ ability to perform fine-grained reasoning in the medical domain.

153 3 PIPELINE

156 This section presents the core pipeline of *MedE*², as illustrated in Figure 2. To enhance the model’s
157 reasoning capabilities, we first curate a high-quality dataset comprising challenging text and multi-
158 modal question-answer pairs (Section 3.1). Based on our pilot studies, we select general MLLMs
159 (e.g., QwenVL-2.5 (Bai et al., 2025b) and InternVL-3.0 (Chen et al., 2024b)) as the base models due
160 to their performance across various medical tasks. Building upon these base models, we propose a
161 two-stage training paradigm that progressively enhances the model’s ability to reason in complex
162 clinical scenarios (Section 3.2 and Section 3.3).

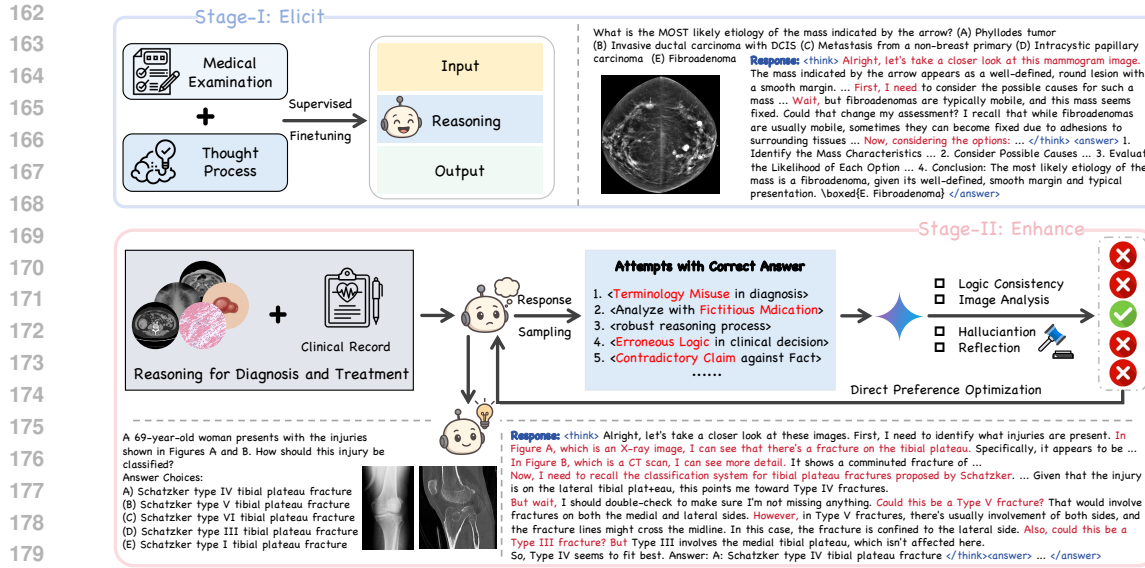


Figure 2: Overview of the two-stage post-training recipe *MedE²*. In Stage-I, text-only data containing reasoning demonstrations is employed to elicit initial reasoning behavior. In Stage-II, Direct Preference Optimization is applied to multimodal data to further enhance reasoning quality.

3.1 DATA COLLECTION

We start with constructing a large-scale question bank sourced from authoritative examinations, top-tier journals, and publicly available datasets. In total, we collect 54K samples, consisting of 37K textual-only and 17K multimodal questions. To ensure high quality and prevent data leakage, a rigorous filtering process was implemented in collaboration with AI experts.

Given that our goal is to explore the potential of multimodal reasoning strategies in solving complex medical tasks, we prioritize filtering out relatively simple samples. Specifically, we employ two baseline models (i.e., QwenVL-2.5 and InternVL-3.0) to eliminate samples that could be solved directly. For multimodal questions, we further prompt Gemini-2.5-Pro to identify the question type and exclude those classified as pattern-recognition tasks. To ensure that the remaining questions are solvable, AI experts independently attempted each question, with 4 attempts per model (Gemini-2.5-pro (Google, 2025) with DeepSeek-R1 (DeepSeek-AI, 2025) for textual questions and Gemini-2.5-pro with Intern-S1 (Bai et al., 2025a) for multimodal questions). Only samples for which both experts answered correctly at least once were retained. Ultimately, this process resulted in a dataset consisting of 5K samples, including 3K textual and 2K multimodal questions.

3.2 STAGE-I: ELICITING REASONING ABILITY

To enable models to effectively reason in clinical problem-solving scenarios, it is essential to instruct them on utilizing their existing knowledge base to address complex reasoning tasks. Previous studies (Ye et al., 2025; Li et al., 2025) have demonstrated that while supervised fine-tuning with reasoning-specific data can enhance reasoning task performance, reasoning capabilities can be elicited effectively with only a few illustrative examples. Indeed, since much of the relevant knowledge has already been encoded during pre-training, the construction of precisely orchestrated demonstrations of reasoning processes is more critical than merely increasing the volume of training data. In this stage, we utilize textual-only reasoning demonstrations to elicit sophisticated reasoning capabilities, rather than relying on multimodal reasoning data. This choice is motivated by empirical findings (Su et al., 2025) that entangled multimodal reasoning data can impair the model’s original language reasoning abilities. In contrast, training exclusively on textual data not only enhances reasoning skills but also maintains general visual understanding, albeit with a slight trade-off.

Building upon prior efforts (Qin et al., 2024; Huang et al., 2024; 2025), we adopt a distillation-based method to generate high-quality reasoning demonstrations using our curated dataset. Specifically, we

leverage state-of-the-art reasoning models, including Gemini-2.5-pro, DeepSeek R1, and Qwen3-235B (Team, 2025), to produce diverse solutions. For open-source models, we directly use their generated reasoning processes. For the proprietary model, such as Gemini-2.5-pro, whose intermediate reasoning steps are not readily accessible, we further prompt gpt-OSS-120B (OpenAI, 2025) to expand its summarized outputs into complete reasoning processes. We conduct rigorous evaluations that combine rule-based filtering with human-assisted validation to ensure the quality of generated solutions. We design three criteria: (i) the correctness of the final answer, (ii) logical structure and organization, and (iii) the plausibility and coherence of the reasoning process. Models trained on our curated textual reasoning data, denoted with the “Stage-I” suffix, demonstrate robust reasoning capabilities, not only in tackling textual domains but also when applied to multimodal scenarios.

3.3 STAGE-II: ENHANCING REASONING QUALITY

Although supervised fine-tuning can elicit reasoning behavior in models, it is often accompanied by an increase in hallucinations. This poses significant risks in medical scenarios, where clinical decision-making requires strong evidence-based justification. Prior work (Lv et al., 2024; Akbar et al., 2024) attributes this phenomenon to a mismatch between the generation paradigms during training and inference. Specifically, models are trained to predict the next token conditioned on preceding ground-truth tokens, while at inference time they rely on their own previously generated outputs. This discrepancy becomes particularly pronounced in tasks requiring long-form reasoning. As illustrated in Figure 2, even a correct answer can emerge from a flawed reasoning process involving terminology misuse, logical errors, or fabricated medical content, etc. To align model outputs with human preference, the mainstream method is to employ Reinforcement Learning from Human Feedback (RLHF) (Ziegler et al., 2019; Ouyang et al., 2022), exemplified by Preference optimization (PO). In this work, we introduce Multimodal Medical Reasoning Preference (MMRP) and integrate it with Direct Preference Optimization (DPO) (Rafailov et al., 2023; Xu et al., 2024). This combination effectively reduces hallucinations and generates reasoning processes that align more closely with user requirements.

Preliminary Considering a model as a policy $\pi_\theta(y|x)$ parameterized by θ , RLHF aims at aligning the LLM π_θ with human preference. DPO is a representative algorithm of RLHF, serving as the preference loss to optimize the policy π_θ by enabling the model to learn the relative preference between chosen and rejected responses. DPO eliminates the requirement of training an explicit reward model based on the assumption of the Bradley-Terry model (Huang et al., 2004) and directly optimizes π_θ :

$$\mathcal{L}_{\text{DPO}}(\pi_\theta) = -\mathbb{E}_{(\mathbf{x}, \mathbf{y}_w, \mathbf{y}_l) \sim \mathcal{D}} \left[\log \sigma \left(\beta \log \frac{\pi_\theta(\mathbf{y}_w | \mathbf{x})}{\pi_{\text{ref}}(\mathbf{y}_w | \mathbf{x})} - \beta \log \frac{\pi_\theta(\mathbf{y}_l | \mathbf{x})}{\pi_{\text{ref}}(\mathbf{y}_l | \mathbf{x})} \right) \right]$$

where \mathbf{y} denotes the response of \mathbf{x} , and $\mathbf{y}_w, \mathbf{y}_l$ represent the “win” and “lose” items in preference pairs. σ is the sigmoid function. π_{ref} is the reference model used to regularize π_θ via Kullback–Leibler divergence, with β controlling the strength of regularization. DPO directly assigns higher probabilities to preferred responses, aligning with human preferences, while bypassing the train-inference mismatch present in SFT.

Multimodal Medical Reasoning Preference

- The reasoning process is logically coherent and step-by-step valid.
- Contain appropriate analysis of relevant visual information.
- Avoid introducing hallucinated content not grounded in the input.
- Includes self-checking, verification, or reflection on uncertainties.

Preference Data Construction. Initially, we prompt the Stage-I model M_1 to generate multiple candidate reasoning processes for each sample in our multimodal training dataset. Given an image I and a question q , we sample candidate reasoning processes y from the distribution $M_1(y | q, I)$, repeating this process 8 times per sample to form a candidate set Y . Notably, each question q undergoes meticulous refinement through collaboration between human experts and a model (GPT-4o), explicitly removing descriptions of image I from q . This ensures that reasoning arises from actual image examination rather than from textual captions. Subsequently, we filter out samples with wrong conclusions and employ Gemini-2.5-Pro to evaluate the remaining candidate reasoning

270 processes according to four MMRP criteria: Logical Consistency, Image Analysis Involvement,
 271 Absence of Hallucinations, and Presence of Reflection. To validate the correctness of the model
 272 judgment, we select 1,000 cases and recruit human annotators to assess them using the same
 273 criteria. The differences between human scores and model judge scores are presented in Figure 3.
 274 We find that model and human evaluations are largely con-
 275 sistent. Reasoning processes meeting all criteria form the
 276 positive set (Y_p), whereas those failing any criteria constitute
 277 the negative set (Y_n). We then construct preference pairs by
 278 selecting a preferred response y_c from Y_p and contrasting it
 279 with a response y_r from Y_n . Unlike static dataset construc-
 280 tion, our MMRP methodology enables dynamic and flexible
 281 curation of multimodal preference datasets, effectively bal-
 282 ancing specialization and generalization in reasoning tasks.
 283 The prompt used for data evaluation with Gemini-2.5-Pro
 284 can be found in Appendix A. Consequently, we obtain 4,432
 285 pairs for QwenVL2.5-7B and 5,224 for InternVL3.0-8B.
 286 After applying DPO-based fine-tuning to the constructed
 287 preference dataset, the model demonstrates improved align-
 288 ment with desired reasoning patterns and shows enhanced
 289 performance across diverse multimodal clinical scenarios.

290 4 EXPERIMENTS

292 4.1 EXPERIMENTAL SETUP

294 We select QwenVL2.5-7B and InternVL3.0-8B as the base models to evaluate the effectiveness
 295 of $MedE^2$, resulting in two variants: (1) +Stage-I, which involves supervised fine-tuning on
 296 text-only data containing reasoning demonstrations; (2) +Stage-II, where the models from Stage-I
 297 are further enhanced using multimodal data and trained with DPO. We report the performance of
 298 GMAI-VL-R1 (Su et al., 2025) and Chiron-o1 (Sun et al., 2025) as baseline methods for comparison.
 299 We also benchmark our approach against state-of-the-art open-source models that operate at substan-
 300 tially larger parameter scales (Bai et al., 2025b; Chen et al., 2024b) and several leading proprietary
 301 models—GPT-4o, OpenAI-o1, Gemini-2.5-Pro, and QvQ-Max (Team). Details of Implementation
 302 can be found in Appendix C.

303 **Evaluation Benchmarks.** Our experiments involve two text-only tasks—MedQA (Jin et al., 2021)
 304 and Medbullets (Chen et al., 2025)—as well as three multimodal benchmarks: MedXpertQA-
 305 MM (Zuo et al., 2025), MMMU-Health (Yue et al., 2024a), and MMMU-Pro-Health (Yue et al.,
 306 2024b). Both MedQA and Medbullets are derived from questions used in the United States Medical
 307 Licensing Examination (USMLE). MedQA includes questions from both Step 1 and Step 2/3 of the
 308 Exam, while Medbullets focuses solely on Step 2/3, which are generally considered more challenging.
 309 For multimodal medical evaluation, MedXpertQA-MM serves as a highly challenging benchmark
 310 that assesses both medical knowledge and reasoning.

311 4.2 MAIN RESULTS

313 **Text-only SFT Elicits Reasoning Behavior.** As shown in Table 4.1, even a limited number of
 314 samples formatted with extended reasoning chains can effectively elicit the reasoning behavior,
 315 resulting in substantial performance gains. For example, QwenVL2.5-7B achieves improvements of
 316 +4.45% on MedXpertQA-MM and +6.67% on MMMU-Health. More impressively, the performance
 317 improvements from reasoning elicitation are even more pronounced for stronger base models. For
 318 example, InternVL3.0-8B achieves an 8% gain on MMMU-Health. This observation aligns with
 319 our hypothesis that training samples can serve as templates, illustrating how to utilize existing
 320 knowledge to solve complex reasoning tasks. Compared to GMAI-VL-R1 SFT, which relies on
 321 10K multimodal samples, our method achieves a 6% increase on MMMU-Health and a 3.37% gain
 322 on MMMU-Pro-Health, using only half of the data in a text-only format. Similarly, relative to
 323 CHIRON-O1, which relies on large-scale supervised fine-tuning with constructed CoT data, $MedE^2$
 324 exhibits a clear performance advantage across all benchmarks. This underscores that high-quality,
 325 task-targeted supervision is more critical than sheer data quantity for developing reasoning abilities.

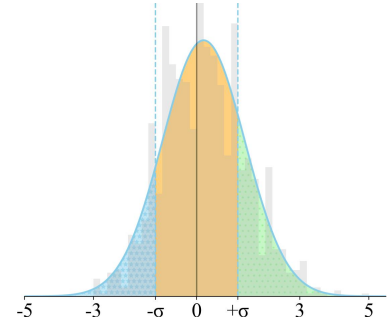


Figure 3: Distribution of human-model score differences, with 68.9% falling within $\pm\sigma$, where $\sigma=1.02$.

324
 325 Table 1: Results (%) of applying *MedE*² to *QwenVL2.5-7B* and *InternVL3.0-8B* on multimodal
 326 medical benchmarks, along with state-of-the-art methods and other training strategies. Δ indicates
 327 the performance gain over the base model, and the best improvements are highlighted in bold.

328 Method	329 MedXpertQA-MM				330 MMMU-Health		331 MMMU-Pro-Health	
	332 Reasoning	333 Understanding	334 Overall	335 Δ	336 Overall	337 Δ	338 Overall	339 Δ
<i>Proprietary</i>								
GPT-4o	40.73	48.19	42.80	–	59.33	–	40.91	–
QvQ-Max	35.20	38.99	36.25	–	70.67	–	52.10	–
OpenAI-o1	52.78	65.45	56.28	–	60.00	–	41.96	–
Gemini-2.5-Pro	61.69	69.13	63.75	–	80.67	–	66.08	–
QwenVL2.5-32B	26.00	30.86	27.35	–	63.33	–	48.25	–
QwenVL2.5-72B	27.10	31.58	28.35	–	70.00	–	50.35	–
InternVL3.0-38B	26.90	29.24	27.55	–	68.00	–	45.10	–
InternVL3.0-78B	28.80	35.92	30.20	–	71.33	–	51.40	–
<i>Baselines</i>								
QwenVL2.5-7B	19.99	22.56	20.70	–	55.33	–	28.47	–
InternVL3.0-8B	21.09	23.83	21.85	–	61.33	–	36.71	–
<i>Advancing</i>								
GMAI-VL-R1 SFT	–	–	23.55	+ 2.85	56.00	+ 0.67	32.99	+ 4.52
GMAI-VL-R1 RLT	–	–	23.80	+ 3.10	57.33	+ 2.00	34.03	+ 5.56
+Stage-I (ours)	24.48	26.90	25.15	+ 4.45	62.00	+ 6.67	36.36	+ 7.89
+Stage-II (ours)	25.80	28.52	26.55	+ 5.85	66.00	+ 10.67	38.81	+ 10.34
Chiron-o1	23.30	25.10	24.20	+ 2.34	54.60	- 6.72	33.90	- 2.80
+Stage-I (ours)	26.14	28.52	26.80	+ 4.95	69.33	+ 8.00	43.36	+ 6.65
+Stage-II (ours)	25.93	31.05	27.35	+ 5.50	70.00	+ 8.67	48.95	+ 12.24

349
 350 **Multimodal DPO Enhances Reasoning Quality.** When Direct Preference Optimization (DPO)
 351 is applied after SFT in Stage-II, it builds upon the structured reasoning patterns established during
 352 the earlier stage and further enhances the model’s output quality. Compared to Group Relative
 353 Policy Optimization (GRPO)-based tuning (Shao et al., 2024) (e.g., GMAI-VL-R1 RLT), our
 354 method achieves notably better results: 26.55% vs. 23.80% on MedXpertQA-MM, 66.00% vs.
 355 57.33% on MMMU-Health, and 38.81% vs. 33.45% on MMMU-Pro-Health. A similar pattern is
 356 also observed in InternVL3.0-8B. These results suggest that merely forcing the model to reason
 357 over limited-solution-space tasks during training is suboptimal, often leading to hallucinations or
 358 incoherent reasoning. Instead, activating reasoning capabilities requires not only complex tasks
 359 but also training samples that engage the model in inference-time computation, or in other words,
 360 examples with precisely orchestrated solutions. Although the performance gain from DPO is slightly
 361 smaller than those from text-only SFT, we observe that DPO helps regulate the issue of “endless
 362 thinking” and encourages the model to “look before it thinks.”

363
 364 **Comparison with State-of-the Art Models.** Table 4.1 also presents a comparison with leading
 365 models. Among open-source models, those enhanced with *MedE*² demonstrate competitive or
 366 even superior performance despite having fewer parameters. For instance, on the MMMU-Health
 367 benchmark, QwenVL2.5-7B with *MedE*² achieves an accuracy of 66%, outperforming its larger coun-
 368 terpart, QwenVL2.5-32B. The performance of InternVL3.0-8B with *MedE*² has already surpassed
 369 InternVL3.0-38B and is slightly lower than InternVL3.0-78B. Similarly, on the MedXpertQA-MM
 370 and MMMU-Pro-Health benchmarks, the smaller models with *MedE*² exhibit performance compara-
 371 ble to that of larger-scale models.

372 4.3 ABLATION STUDIES

373
 374 **Larger Models, Greater Improvements** Based on the preceding results, we observe that models
 375 exhibiting stronger initial performance tend to benefit more from reasoning elicitation. We hypo-
 376 thesize that larger models equipped with more extensive pretrained knowledge can derive increased
 377 benefits from our proposed *MedE*² framework. To rigorously verify this hypothesis, we apply our
 378 training pipeline to QwenVL2.5-32B and QwenVL2.5-72B and evaluate them on MedXpertQA-
 379 MM. We select MedXpertQA-MM for evaluation due to its increased challenge and minimal data
 380 leakage risk, as it was carefully constructed using difficulty-based filtering and data augmentation.

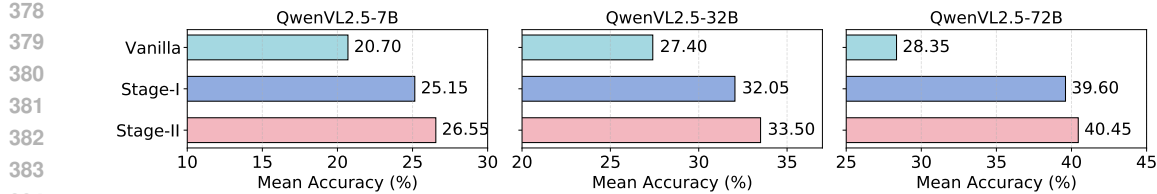


Figure 4: The performance of QwenVL2.5-7B, 32B and 72B on the MedXpertQA-MM benchmark. As the model size increases, the models demonstrate progressively greater benefits from the *MedE*².

Figure 4 illustrates the accuracy variations across different model sizes at various stages. Following Stage-I, QwenVL2.5-72B demonstrates the most substantial performance gain, outperforming both QwenVL2.5-32B (4.65%) and QwenVL2.5-7B (4.45%). These findings are consistent with our assumption in Section 3.2: models with more extensive prerequisite knowledge encoded within their parameter space are more capable of learning reasoning patterns from limited yet precisely structured exemplars. Combining the results shown in Table 4.1, we surprisingly find that QwenVL2.5-72B enhanced with *MedE*² even surpasses QvQ-Max (40.45% versus 36.25%) on the MedXpertQA-MM benchmark, which is currently one of the most powerful models within the Qwen series. Although larger proprietary models such as o1 and Gemini-2.5-Pro still maintain an advantage on challenging benchmarks, the application of *MedE*² significantly narrows the performance gap between open-source and proprietary models. These results further demonstrate the effectiveness of *MedE*² in advancing multimodal reasoning capabilities for medical tasks. Detailed experimental results can be found in Appendix D.

Text-only vs. Multimodal Elicitation. Previous studies have attempted to utilize multimodal training samples to activate multimodal reasoning capabilities. However, models optimized with such data often suffer from performance degradation on general vision tasks and impairment in linguistic abilities. Specifically, we compare text-only SFT, multimodal SFT, and their combination within Stage-I. In addition to evaluating on multimodal benchmarks (MedXpertQA-MM and MMMU-Health), we also assess performance on two language-focused benchmarks: MedQA and Medbullets. As illustrated in Figure 5, both text-only and multimodal SFT successfully elicit reasoning behaviors and improve overall performance. However, multimodal SFT yields relatively smaller improvements compared to text-only SFT. Notably, combining text-only and multimodal SFT results in reduced performance compared to the text-only SFT setting, particularly evident in the text tasks. This finding confirms that eliciting reasoning abilities through multimodal data may compromise the original language capabilities of the model.

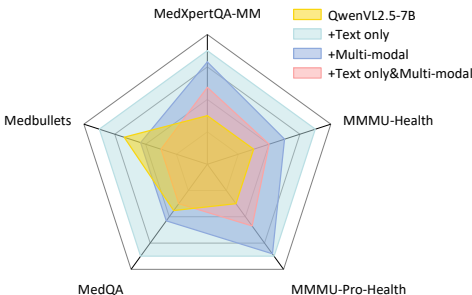


Figure 5: Comparison of performance on MedXpertQA-MM using various strategies for eliciting reasoning behaviors.

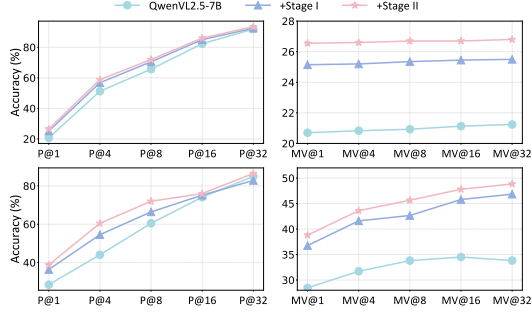


Figure 6: The Accuracy of models with *MedE*² on MedXpertQA-MM (upper part) and MMMU-Pro-Health (lower part) with inference-time scaling.

Benefit when Applying Inference Time Scaling. To investigate the effectiveness of *MedE*², in scaling up inference time, we report the results of majority-vote accuracy and pass@n accuracy on MedXpertQA-MM and MMMU-Pro-Health across 32 computational runs with temperature=0.5. The results, illustrated in Figure 6, compare the performance of three models under Pass@n and majority voting (MV@n). Since both datasets are in a multiple-choice format with a limited answer

432 A 6-year-old boy presents with a forearm
 433 deformity, and radiographs in Figure A confirm the
 434 diagnosis. What additional diagnostic tests should
 435 be performed for this patient?
 436

437 **Answer Choices:**
 438 (A) CBC, renal ultrasound, and echocardiogram
 439 (B) CBC and MRI
 440 (C) CBC and renal ultrasound only
 441 (D) No additional testing needed
 442 (E) CBC

443

444

445

446

447

448

449

450

451

452

453

454

455

456

457

458

459

460

461

462

463

464

465

466

467

468

469

470

471

472

473

474

475

476

477

478

479

480

481

482

483

484

485

486

487

488

489

490

491

492

493

494

495

496

497

498

499

500

501

502

503

504

505

506

507

508

509

510

511

512

513

514

515

516

517

518

519

520

521

522

523

524

525

526

527

528

529

530

531

532

533

534

535

536

537

538

539

540

541

542

543

544

545

546

547

548

549

550

551

552

553

554

555

556

557

558

559

560

561

562

563

564

565

566

567

568

569

570

571

572

573

574

575

576

577

578

579

580

581

582

583

584

585

586

587

588

589

590

591

592

593

594

595

596

597

598

599

600

601

602

603

604

605

606

607

608

609

610

611

612

613

614

615

616

617

618

619

620

621

622

623

624

625

626

627

628

629

630

631

632

633

634

635

636

637

638

639

640

641

642

643

644

645

646

647

648

649

650

651

652

653

654

655

656

657

658

659

660

661

662

663

664

665

666

667

668

669

670

671

672

673

674

675

676

677

678

679

680

681

682

683

684

685

686

687

688

689

690

691

692

693

694

695

696

697

698

699

700

701

702

703

704

705

706

707

708

709

710

711

712

713

714

715

716

717

718

719

720

721

722

723

724

725

726

727

728

729

730

731

732

733

734

735

736

737

738

739

740

741

742

743

744

745

746

747

748

749

750

751

752

753

754

755

756

757

758

759

760

761

762

763

764

765

766

767

768

769

770

771

772

773

774

775

776

777

778

779

780

781

782

783

784

785

786

787

788

789

790

791

792

793

794

795

796

797

798

799

800

801

802

803

804

805

806

807

808

809

810

811

812

813

814

815

816

817

818

819

820

821

822

823

824

825

826

827

828

829

830

831

832

833

834

835

836

837

838

839

840

841

842

843

844

845

846

847

848

849

850

851

852

853

854

855

856

857

858

859

860

861

862

863

864

865

866

867

868

869

870

871

872

873

874

875

876

877

878

879

880

881

882

883

884

885

886

887

888

889

890

891

892

893

894

895

896

897

898

899

900

901

902

903

904

905

906

907

908

909

910

911

912

913

914

915

916

917

918

919

920

921

922

923

924

925

926

927

928

929

930

931

932

933

934

935

936

937

938

939

940

941

942

943

944

945

946

947

948

949

950

951

952

953

954

955

956

957

958

959

960

961

962

963

964

965

966

967

968

969

970

971

972

973

974

975

976

977

978

979

980

981

982

983

984

985

986

987

988

989

990

991

992

993

994

995

996

997

998

999

1000

1001

1002

1003

1004

1005

1006

1007

1008

1009

1010

1011

1012

1013

1014

1015

1016

1017

1018

1019

1020

1021

1022

1023

1024

1025

1026

1027

1028

1029

1030

1031

1032

1033

1034

1035

1036

1037

1038

1039

1040

1041

1042

1043

1044

1045

1046

1047

1048

1049

1050

1051

1052

1053

1054

1055

1056

1057

1058

1059

1060

1061

1062

1063

1064

1065

1066

1067

1068

1069

1070

1071

1072

1073

1074

1075

1076

1077

1078

1079

1080

1081

1082

1083

1084

1085

1086

1087

1088

1089

1090

1091

1092

1093

1094

1095

1096

1097

1098

1099

1100

1101

1102

1103

1104

1105

1106

1107

1108

1109

1110

1111

1112

1113

1114

1115

1116

1117

1118

1119

1120

1121

1122

1123

1124

1125

1126

1127

1128

1129

1130

1131

1132

1133

1134

1135

1136

1137

1138

1139

1140

1141

1142

1143

1144

1145

1146

1147

1148

1149

1150

1151

1152

1153

1154

1155

1156

1157

1158

1159

1160

1161

1162

1163

1164

1165

1166

1167

1168

1169

1170

1171

1172

1173

1174

1175

1176

1177

1178

1179

1180

1181

1182

1183

1184

1185

1186

1187

1188

1189

1190

1191

1192

1193

1194

1195

1196

1197

1198

1199

1200

1201

1202

1203

1204

1205

1206

1207

1208

1209

1210

1211

1212

1213

1214

1215

1216

1217

1218

1219

1220

1221

1222

1223

1224

1225

1226

1227

1228

1229

1230

1231

1232

1233

1234

1235

1236

1237

1238

1239

1240

1241

1242

1243

1244

1245

1246

1247

1248

1249

1250

1251

1252

1253

1254

1255

1256

1257

1258

1259

1260

1261

1262

1263

1264

1265

1266

1267

1268

1269

1270

1271

1272

1273

1274

1275

1276

1277

1278

1279

1280

1281

1282

1283

1284

1285

1286

1287

1288

1289

1290

1291

1292

1293

1294

1295

1296

1297

1298

1299

1300

1301

1302

1303

1304

1305

1306

1307

1308

1309

1310

1311

1312

1313

1314

1315

1316

1317

1318

1319

1320

1321

1322

1323

1324

1325

1326

1327

1328

1329

1330

1331

1332

1333

1334

1335

1336

1337

1338

1339

1340

1341

1342

1343

1344

1345

1346

1347

1348

1349

1350

1351

1352

1353

1354

1355

1356

1357

1358

1359

1360

1361

1362

1363

1364

1365

1366

1367

1368

1369

1370

1371

1372

1373

1374

1375

1376

1377

1378

1379

1380

1381

1382

1383

1384

1385

1386

1387

1388

1389

1390

1391

1392

1393

1394

1395

1396

1397

1398

1399

1400

1401

1402

1403

1404

1405

1406

1407

1408

1409

1410

1411

1412

1413

1414

1415

1416

1417

1418

1419

1420

1421

1422

1423

1424

1425

1426

1427

1428

1429

1430

1431

1432

1433

1434

1435

1436

1437

1438

1439

1440

1441

1442

1443

1444

1445

1446

1447

1448

1449

1450

1451

1452

1453

1454

1455

1456

1457

1458

1459

1460

1461

1462

1463

1464

1465

1466

1467

1468

1469

1470

1471

1472

1473

1474

1475

1476

1477

1478

1479

1480

1481

1482

1483

1484

1485

1486

1487

1488

1489

1490

1491

1492

1493

1494

1495

1496

1497

1498

1499

1500

1501

1502

1503

1504

1505

1506

1507

1508

1509

1510

1511

1512

1513

1514

1515

1516

1517

1518

1519

1520

1521

1522

1523

1524

1525

1526

1527

1528

1529

1530

1531

1532

1533

1534

1535

1536

1537

1538

1539

1540

1541

1542

1543

1544

1545

1546

1547

1548

1549

1550

1551

1552

1553

1554

1555

1556

1557

1558

1559

1560

1561

1562

1563

1564

1565

1566

1567

1568

1569

1570

1571

1572

1573

1574

1575

1576

1577

1578

1579

1580

1581

1582

1583

1584

1585

1586

1587

1588

1589

1590

1591

1592

1593

1594

1595

1596

1597

1598

1599

1600

1601

1602

1603

1604

1605

1606

1607

1608

1609

1610

1611

1612

1613

1614

1615

1616

1617

1618

1619

1620

1621

1622

1623

1624

1625

1626

1627

1628

1629

1630

1631

1632

1633

1634

1635

1636

1637

1638

1639

1640

1641

1642

1643

1644

1645

1646

1647

1648

1649

1650

1651

1652

1653

1654

1655

1656

1657

1658

1659

1660

1661

1662

1663

1664

1665

1666

1667

1668

1669

1670

1671

1672

1673

1674

1675

1676

1677

1678

1679

1680

1681

1682

1683

1684

1685

1686

1687

1688

1689

1690

1691

1692

1693

1694

1695

1696

1697

1698

1699

1700

1701

1702

1703

1704

1705

1706

1707

1708

1709

1710

1711

1712

1713

1714

1715

1716

1717

1718

1719

1720

1721

1722

1723

1724

1725

1726

1727

1728

1729

1730

1731

1732

1733

1734

1735

1736

1737

1738

1739

1740

1741

1742

1743

1744

<p

486 ETHICS STATEMENT
487

488 This work complies fully with the ICLR Code of Ethics. All datasets used in this paper are publicly
489 available and were obtained from established open sources. No private, sensitive, or personally
490 identifiable information was collected or used. The study involves no human subjects, no experiments
491 on vulnerable populations, and no interventions requiring IRB approval. We confirm that our
492 methodology and results do not raise foreseeable risks of harm, misuse, or ethical concerns beyond
493 standard scientific research practices.

494 REPRODUCIBILITY STATEMENT
495

496 We will open-source the curated dataset and model weights at <https://anonymous.4open.science/r/MedEE-C381> to facilitate reproduction. We provide a comprehensive overview of
497 our data construction methodology, the full processing pipeline, and the specific prompts used are
498 provided in Appendix A. In addition, the training details and hyperparameter configurations for both
499 stages of our method are presented in Appendix C.

501
502 REFERENCES
503

504 Julia Adler-Milstein, Jonathan H Chen, and Gurpreet Dhaliwal. Next-generation artificial intelligence
505 for diagnosis: From predicting diagnostic labels to “wayfinding”. *JAMA*, 326(24):2467–2468,
506 2021.

507 Shayan Ali Akbar, Md Mosharaf Hossain, Tess Wood, Si-Chi Chin, Erica Salinas, Victor Alvarez, and
508 Erwin Cornejo. Hallumeasure: Fine-grained hallucination measurement using chain-of-thought
509 reasoning. In *Proceedings of the 2024 Conference on Empirical Methods in Natural Language
510 Processing*, pp. 15020–15037, 2024.

511 Lei Bai, Zhongrui Cai, Maosong Cao, Weihan Cao, Chiyu Chen, Haojiong Chen, Kai Chen,
512 Pengcheng Chen, Ying Chen, Yongkang Chen, Yu Cheng, Yu Cheng, Pei Chu, Tao Chu, Er-
513 fei Cui, Ganqu Cui, Long Cui, Ziyun Cui, Nianchen Deng, Ning Ding, Nanqin Dong, Peijie Dong,
514 Shihan Dou, Sinan Du, Haodong Duan, Caihua Fan, Ben Gao, Changjiang Gao, Jianfei Gao,
515 Songyang Gao, Yang Gao, Zhangwei Gao, Jiaye Ge, Qiming Ge, Lixin Gu, Yuzhe Gu, Aijia Guo,
516 Qipeng Guo, Xu Guo, Conghui He, Junjun He, Yili Hong, Siyuan Hou, Caiyu Hu, Hanglei Hu,
517 Jucheng Hu, Ming Hu, Zhouqi Hua, Haian Huang, Junhao Huang, Xu Huang, Zixian Huang, Zhe
518 Jiang, Lingkai Kong, Linyang Li, Peiji Li, Pengze Li, Shuaibin Li, Tianbin Li, Wei Li, Yuqiang Li,
519 Dahua Lin, Junyao Lin, Tianyi Lin, Zhishan Lin, Hongwei Liu, Jiangning Liu, Jiyao Liu, Junnan
520 Liu, Kai Liu, Kaiwen Liu, Kuikun Liu, Shichun Liu, Shudong Liu, Wei Liu, Xinyao Liu, Yuhong
521 Liu, Zhan Liu, Yinquan Lu, Haijun Lv, Hongxia Lv, Huijie Lv, Qidang Lv, Ying Lv, Chengqi Lyu,
522 Chenglong Ma, Jianpeng Ma, Ren Ma, Runmin Ma, Runyuan Ma, Xinzhu Ma, Yichuan Ma, Zihan
523 Ma, Sixuan Mi, Junzhi Ning, Wenchang Ning, Xinle Pang, Jiahui Peng, Runyu Peng, Yu Qiao,
524 Jiantao Qiu, Xiaoye Qu, Yuan Qu, Yuchen Ren, Fukai Shang, Wenqi Shao, Junhao Shen, Shuaike
525 Shen, Chunfeng Song, Demin Song, Diping Song, Chenlin Su, Weijie Su, Weigao Sun, Yu Sun,
526 Qian Tan, Cheng Tang, Huanze Tang, Kexian Tang, Shixiang Tang, Jian Tong, Aoran Wang, Bin
527 Wang, Dong Wang, Lintao Wang, Rui Wang, Weiyun Wang, Wenhui Wang, Yi Wang, Ziyi Wang,
528 Ling-I Wu, Wen Wu, Yue Wu, Zijian Wu, Linchen Xiao, Shuhao Xing, Chao Xu, Huihui Xu, Jun
529 Xu, Ruiliang Xu, Wanghan Xu, GanLin Yang, Yuming Yang, Haochen Ye, Jin Ye, Shenglong Ye,
530 Jia Yu, Jiashuo Yu, Jing Yu, Fei Yuan, Bo Zhang, Chao Zhang, Chen Zhang, Hongjie Zhang, Jin
531 Zhang, Qiaosheng Zhang, Qiuyinzhe Zhang, Songyang Zhang, Taolin Zhang, Wenlong Zhang,
532 Wenwei Zhang, Yechen Zhang, Ziyang Zhang, Haiteng Zhao, Qian Zhao, Xiangyu Zhao, Xiangyu
533 Zhao, Bowen Zhou, Dongzhan Zhou, Peiheng Zhou, Yuhao Zhou, Yunhua Zhou, Dongsheng Zhu,
534 Lin Zhu, and Yicheng Zou. Intern-s1: A scientific multimodal foundation model, 2025a. URL
535 <https://arxiv.org/abs/2508.15763>.

536 Shuai Bai, Keqin Chen, Xuejing Liu, Jialin Wang, Wenbin Ge, Sibo Song, Kai Dang, Peng Wang,
537 Shijie Wang, Jun Tang, et al. Qwen2. 5-vl technical report. *arXiv preprint arXiv:2502.13923*,
538 2025b.

539 Hanjie Chen, Zhouxiang Fang, Yash Singla, and Mark Dredze. Benchmarking large language
models on answering and explaining challenging medical questions. In *Proceedings of the*

540 2025 Conference of the Nations of the Americas Chapter of the Association for Computational
 541 Linguistics: Human Language Technologies (Volume 1: Long Papers), pp. 3563–3599, 2025.

542

543 Junying Chen, Chi Gui, Ruyi Ouyang, Anningzhe Gao, Shunian Chen, Guiming Hardy Chen, Xidong
 544 Wang, Ruifei Zhang, Zhenyang Cai, Ke Ji, et al. Huatuogpt-vision, towards injecting medical
 545 visual knowledge into multimodal llms at scale. [arXiv preprint arXiv:2406.19280](https://arxiv.org/abs/2406.19280), 2024a.

546

547 Zhe Chen, Jiannan Wu, Wenhui Wang, Weijie Su, Guo Chen, Sen Xing, Muyan Zhong, Qinglong
 548 Zhang, Xizhou Zhu, Lewei Lu, et al. Internvl: Scaling up vision foundation models and aligning
 549 for generic visual-linguistic tasks. In [Proceedings of the IEEE/CVF Conference on Computer
 Vision and Pattern Recognition](https://openaccess.thecvf.com/content/CVPR2024/papers/Internvl_Scaling_up_Vision_Foundation_Models_and_aligning_for_Generic_Visual-Linguistic_Tasks_CVPR_2024_paper.pdf), pp. 24185–24198, 2024b.

550

551 Pat Croskerry and Mike Clancy. Advancing diagnostic excellence: the cognitive challenge for
 552 medicine. [BMJ](https://bmj.com/content/376/0/799), 376:0799, 2022.

553

554 DeepSeek-AI. Deepseek-r1: Incentivizing reasoning capability in llms via reinforcement learning,
 555 2025. URL <https://arxiv.org/abs/2501.12948>.

556

557 Danny Driess, Fei Xia, Mehdi SM Sajjadi, Corey Lynch, Aakanksha Chowdhery, Ayzaan Wahid,
 558 Jonathan Tompson, Quan Vuong, Tianhe Yu, Wenlong Huang, et al. Palm-e: An embodied
 559 multimodal language model. 2023.

560

561 Google. Gemini-2.5-pro. <https://gemini.google.com>, 2025. Accessed: May 2025.

562

563 Edward J Hu, Yelong Shen, Phillip Wallis, Zeyuan Allen-Zhu, Yuanzhi Li, Shean Wang, Lu Wang,
 564 Weizhu Chen, et al. Lora: Low-rank adaptation of large language models. [ICLR](https://openaccess.thecvf.com/content/ICLR2022/track2/123.pdf), 1(2):3, 2022.

565

566 Tzu-Kuo Huang, Chih-Jen Lin, and Ruby Weng. A generalized bradley-terry model: From group
 567 competition to individual skill. [Advances in neural information processing systems](https://openaccess.thecvf.com/content/ICLR2004/track2/17.pdf), 17, 2004.

568

569 Zhen Huang, Haoyang Zou, Xuefeng Li, Yixiu Liu, Yuxiang Zheng, Ethan Chern, Shijie Xia, Yiwei
 570 Qin, Weizhe Yuan, and Pengfei Liu. O1 replication journey–part 2: Surpassing o1-preview through
 571 simple distillation, big progress or bitter lesson? [arXiv preprint arXiv:2411.16489](https://arxiv.org/abs/2411.16489), 2024.

572

573 Zhongzhen Huang, Gui Geng, Shengyi Hua, Zhen Huang, Haoyang Zou, Shaoting Zhang, Pengfei
 574 Liu, and Xiaofan Zhang. O1 replication journey – part 3: Inference-time scaling for medical
 575 reasoning. [arXiv preprint arXiv:2501.06458](https://arxiv.org/abs/2501.06458), 2025.

576

577 Di Jin, Eileen Pan, Nassim Oufattolle, Wei-Hung Weng, Hanyi Fang, and Peter Szolovits. What
 578 disease does this patient have? a large-scale open domain question answering dataset from medical
 579 exams. [Applied Sciences](https://openaccess.thecvf.com/content/ICLR2021/track2/11.pdf), 11(14):6421, 2021.

580

581 Woosuk Kwon, Zhuohan Li, Siyuan Zhuang, Ying Sheng, Lianmin Zheng, Cody Hao Yu, Joseph E.
 582 Gonzalez, Hao Zhang, and Ion Stoica. Efficient memory management for large language model
 583 serving with pagedattention. In [Proceedings of the ACM SIGOPS 29th Symposium on Operating
 584 Systems Principles](https://openaccess.thecvf.com/content/ICLR2023/track2/29.pdf), 2023.

585

586 Yuxiang Lai, Jike Zhong, Ming Li, Shitian Zhao, and Xiaofeng Yang. Med-r1: Reinforcement learning
 587 for generalizable medical reasoning in vision-language models. [arXiv preprint arXiv:2503.13939](https://arxiv.org/abs/2503.13939),
 588 2025.

589

590 Jason J Lau, Soumya Gayen, Asma Ben Abacha, and Dina Demner-Fushman. A dataset of clinically
 591 generated visual questions and answers about radiology images. [Scientific data](https://openaccess.thecvf.com/content/ICLR2018/track2/5.pdf), 5(1):1–10, 2018.

592

593 Chunyuan Li, Cliff Wong, Sheng Zhang, Naoto Usuyama, Haotian Liu, Jianwei Yang, Tristan
 594 Naumann, Hoifung Poon, and Jianfeng Gao. Llava-med: Training a large language-and-vision
 595 assistant for biomedicine in one day. [Advances in Neural Information Processing Systems](https://openaccess.thecvf.com/content/ICLR2023/track2/36.pdf), 36:
 596 28541–28564, 2023.

597

598 Xuefeng Li, Haoyang Zou, and Pengfei Liu. Limr: Less is more for rl scaling. [arXiv preprint
 599 arXiv:2502.11886](https://arxiv.org/abs/2502.11886), 2025.

600

601 Yuan Li, Xiaodan Liang, Zhitong Hu, and Eric P Xing. Hybrid retrieval-generation reinforced agent
 602 for medical image report generation. [Advances in neural information processing systems](https://openaccess.thecvf.com/content/ICLR2018/track2/31.pdf), 31,
 603 2018.

594 Bo Liu, Li-Ming Zhan, Li Xu, Lin Ma, Yan Yang, and Xiao-Ming Wu. Slake: A semantically-
 595 labeled knowledge-enhanced dataset for medical visual question answering. In 2021 IEEE 18th
 596 international symposium on biomedical imaging (ISBI), pp. 1650–1654. IEEE, 2021.

597

598 Renqian Luo, Lai Sun, Yingce Xia, Tao Qin, Sheng Zhang, Hoifung Poon, and Tie-Yan Liu.
 599 Biogpt: generative pre-trained transformer for biomedical text generation and mining. Briefings in
 600 bioinformatics, 23(6):bbac409, 2022.

601

602 Qitan Lv, Jie Wang, Hanzhu Chen, Bin Li, Yongdong Zhang, and Feng Wu. Coarse-to-fine
 603 highlighting: Reducing knowledge hallucination in large language models. arXiv preprint
 604 arXiv:2410.15116, 2024.

605

606 Fanqing Meng, Lingxiao Du, Zongkai Liu, Zhixiang Zhou, Quanfeng Lu, Daocheng Fu, Tiancheng
 607 Han, Botian Shi, Wenhui Wang, Junjun He, et al. Mm-eureka: Exploring the frontiers of multimodal
 608 reasoning with rule-based reinforcement learning. arXiv preprint arXiv:2503.07365, 2025.

609

610 Yingqian Min, Zhipeng Chen, Jinhao Jiang, Jie Chen, Jia Deng, Yiwen Hu, Yiru Tang, Jiapeng Wang,
 611 Xiaoxue Cheng, Huatong Song, et al. Imitate, explore, and self-improve: A reproduction report on
 612 slow-thinking reasoning systems. arXiv preprint arXiv:2412.09413, 2024.

613

614 OpenAI. Learning to reason with llms, 2024. URL <https://openai.com/index-learning-to-reason-with-llms>.

615

616 OpenAI. gpt-oss-120b gpt-oss-20b model card, 2025. URL <https://arxiv.org/abs/2508.10925>.

617

618 Long Ouyang, Jeffrey Wu, Xu Jiang, Diogo Almeida, Carroll Wainwright, Pamela Mishkin, Chong
 619 Zhang, Sandhini Agarwal, Katarina Slama, Alex Ray, et al. Training language models to follow
 620 instructions with human feedback. Advances in neural information processing systems, 35:27730–
 27744, 2022.

621

622 Jiazen Pan, Che Liu, Junde Wu, Fenglin Liu, Jiayuan Zhu, Hongwei Bran Li, Chen Chen, Cheng
 623 Ouyang, and Daniel Rueckert. Medvilm-r1: Incentivizing medical reasoning capability of vision-
 624 language models (vlms) via reinforcement learning. arXiv preprint arXiv:2502.19634, 2025.

625

626 PubMed. Pmc open access subset [internet]. <https://pmc.ncbi.nlm.nih.gov/tools/openftlist/>, 2003. Bethesda (MD): National Library of Medicine. [cited 2025 Sep 16].

627

628 Yiwei Qin, Xuefeng Li, Haoyang Zou, Yixiu Liu, Shijie Xia, Zhen Huang, Yixin Ye, Weizhe Yuan,
 629 Hector Liu, Yuanzhi Li, et al. O1 replication journey: A strategic progress report–part 1. arXiv
 630 preprint arXiv:2410.18982, 2024.

631

632 Rafael Rafailov, Archit Sharma, Eric Mitchell, Christopher D Manning, Stefano Ermon, and Chelsea
 633 Finn. Direct preference optimization: Your language model is secretly a reward model. Advances
 634 in Neural Information Processing Systems, 36:53728–53741, 2023.

635

636 Jeff Rasley, Samyam Rajbhandari, Olatunji Ruwase, and Yuxiong He. Deepspeed: System opti-
 637 mizations enable training deep learning models with over 100 billion parameters. In Proceedings
 638 of the 26th ACM SIGKDD international conference on knowledge discovery & data mining, pp.
 3505–3506, 2020.

639

640 Khaled Saab, Tao Tu, Wei-Hung Weng, Ryutaro Tanno, David Stutz, Ellery Wulczyn, Fan Zhang,
 641 Tim Strother, Chunjong Park, Elahe Vedadi, et al. Capabilities of gemini models in medicine.
 642 arXiv preprint arXiv:2404.18416, 2024.

643

644 Marc Cicero Schubert, Maximilian Lasotta, Felix Sahm, Wolfgang Wick, and Varun Venkataramani.
 645 Evaluating the multimodal capabilities of generative ai in complex clinical diagnostics. Medrxiv,
 646 pp. 2023–11, 2023.

647

Zhihong Shao, Peiyi Wang, Qihao Zhu, Runxin Xu, Junxiao Song, Xiao Bi, Haowei Zhang,
 648 Mingchuan Zhang, YK Li, Y Wu, et al. Deepseekmath: Pushing the limits of mathematical
 649 reasoning in open language models. arXiv preprint arXiv:2402.03300, 2024.

648 Hardeep Singh, Denise M Connor, and Gurpreet Dhaliwal. Five strategies for clinicians to advance
 649 diagnostic excellence. [BMJ](#), 376:e068044, 2022.
 650

651 Yanzhou Su, Tianbin Li, Jiyao Liu, Chenglong Ma, Junzhi Ning, Cheng Tang, Sibo Ju, Jin Ye,
 652 Pengcheng Chen, Ming Hu, et al. Gmai-vl-r1: Harnessing reinforcement learning for multimodal
 653 medical reasoning. [arXiv preprint arXiv:2504.01886](#), 2025.

654 Haoran Sun, Yankai Jiang, Wenjie Lou, Yujie Zhang, Wenjie Li, Lilong Wang, Mianxin Liu, Lei Liu,
 655 and Xiaosong Wang. Enhancing step-by-step and verifiable medical reasoning in mllms. [arXiv](#)
 656 [preprint arXiv:2506.16962](#), 2025.
 657

658 Qwen Team. Qvq-max: Think with evidence.
 659

660 Qwen Team. Qwen3 technical report, 2025. URL <https://arxiv.org/abs/2505.09388>.
 661

662 Tao Tu, Shekoofeh Azizi, Danny Driess, Mike Schaekermann, Mohamed Amin, Pi-Chuan Chang,
 663 Andrew Carroll, Charles Lau, Ryutaro Tanno, Ira Ktena, et al. Towards generalist biomedical ai.
 664 [Nejm Ai](#), 1(3):A10a2300138, 2024.

665 Weiyun Wang, Zhe Chen, Wenhui Wang, Yue Cao, Yangzhou Liu, Zhangwei Gao, Jinguo Zhu,
 666 Xizhou Zhu, Lewei Lu, Yu Qiao, et al. Enhancing the reasoning ability of multimodal large
 667 language models via mixed preference optimization. [arXiv preprint arXiv:2411.10442](#), 2024.

668 Jason Wei, Xuezhi Wang, Dale Schuurmans, Maarten Bosma, Fei Xia, Ed Chi, Quoc V Le, Denny
 669 Zhou, et al. Chain-of-thought prompting elicits reasoning in large language models. [Advances in](#)
 670 [neural information processing systems](#), 35:24824–24837, 2022.
 671

672 Yichen Wei, Yi Peng, Xiaokun Wang, Weijie Qiu, Wei Shen, Tianyidan Xie, Jiangbo Pei, Jianhao
 673 Zhang, Yunzhuo Hao, Xuchen Song, et al. Skywork r1v2: Multimodal hybrid reinforcement
 674 learning for reasoning. [arXiv preprint arXiv:2504.16656](#), 2025.

675 Yunfei Xie, Ce Zhou, Lang Gao, Juncheng Wu, Xianhang Li, Hong-Yu Zhou, Sheng Liu, Lei Xing,
 676 James Zou, Cihang Xie, et al. Medtrinity-25m: A large-scale multimodal dataset with multigranular
 677 annotations for medicine. [arXiv preprint arXiv:2408.02900](#), 2024.
 678

679 Shusheng Xu, Wei Fu, Jiaxuan Gao, Wenjie Ye, Weilin Liu, Zhiyu Mei, Guangju Wang, Chao Yu,
 680 and Yi Wu. Is dpo superior to ppo for llm alignment? a comprehensive study. [arXiv preprint](#)
 681 [arXiv:2404.10719](#), 2024.

682 Shunyu Yao, Jeffrey Zhao, Dian Yu, Nan Du, Izhak Shafran, Karthik Narasimhan, and Yuan Cao.
 683 React: Synergizing reasoning and acting in language models. In [International Conference on](#)
 684 [Learning Representations \(ICLR\)](#), 2023.
 685

686 Qichen Ye, Junling Liu, Dading Chong, Peilin Zhou, Yining Hua, Fenglin Liu, Meng Cao, Ziming
 687 Wang, Xuxin Cheng, Zhu Lei, et al. Qilin-med: Multi-stage knowledge injection advanced medical
 688 large language model. [arXiv preprint arXiv:2310.09089](#), 2023.

689 Yixin Ye, Zhen Huang, Yang Xiao, Ethan Chern, Shijie Xia, and Pengfei Liu. Limo: Less is more for
 690 reasoning. [arXiv preprint arXiv:2502.03387](#), 2025.
 691

692 Xiang Yue, Yuansheng Ni, Kai Zhang, Tianyu Zheng, Ruqi Liu, Ge Zhang, Samuel Stevens, Dongfu
 693 Jiang, Weiming Ren, Yuxuan Sun, et al. Mmmu: A massive multi-discipline multimodal under-
 694 standing and reasoning benchmark for expert agi. In [Proceedings of the IEEE/CVF Conference](#)
 695 [on Computer Vision and Pattern Recognition](#), pp. 9556–9567, 2024a.

696 Xiang Yue, Tianyu Zheng, Yuansheng Ni, Yubo Wang, Kai Zhang, Shengbang Tong, Yuxuan Sun,
 697 Botao Yu, Ge Zhang, Huan Sun, et al. Mmmu-pro: A more robust multi-discipline multimodal
 698 understanding benchmark. [arXiv preprint arXiv:2409.02813](#), 2024b.
 699

700 Kai Zhang, Rong Zhou, Eashan Adhikarla, Zhiling Yan, Yixin Liu, Jun Yu, Zhengliang Liu, Xun
 701 Chen, Brian D Davison, Hui Ren, et al. A generalist vision–language foundation model for diverse
 biomedical tasks. [Nature Medicine](#), pp. 1–13, 2024.

702 Yaowei Zheng, Richong Zhang, Junhao Zhang, Yanhan Ye, Zheyuan Luo, Zhangchi Feng, and
703 Yongqiang Ma. Llamafactory: Unified efficient fine-tuning of 100+ language models. In
704 Proceedings of the 62nd Annual Meeting of the Association for Computational Linguistics
705 (Volume 3: System Demonstrations), Bangkok, Thailand, 2024. Association for Computational
706 Linguistics. URL <http://arxiv.org/abs/2403.13372>.

707 Daniel M Ziegler, Nisan Stiennon, Jeffrey Wu, Tom B Brown, Alec Radford, Dario Amodei, Paul
708 Christiano, and Geoffrey Irving. Fine-tuning language models from human preferences. arXiv
709 preprint arXiv:1909.08593, 2019.

711 Yuxin Zuo, Shang Qu, Yifei Li, Zhangren Chen, Xuekai Zhu, Ermo Hua, Kaiyan Zhang, Ning Ding,
712 and Bowen Zhou. Medxpertqa: Benchmarking expert-level medical reasoning and understanding.
713 arXiv preprint arXiv:2501.18362, 2025.

714

715

716

717

718

719

720

721

722

723

724

725

726

727

728

729

730

731

732

733

734

735

736

737

738

739

740

741

742

743

744

745

746

747

748

749

750

751

752

753

754

755

756 A PROMPT TEMPLATES AND DATA FORMATS ADOPTED IN *MedE*²
757758 The format of the text-only SFT data in Stage-I
759

```

760 "messages": [
761   {
762     "role": "system",
763     "content": "You are a helpful assistant. A conversation between
764     User and Assistant. The user asks a question, and the Assistant
765     solves it. The assistant first thinks about the reasoning proc-
766     ess in the mind and then provides the user with the answer. The
767     reasoning process and answer are enclosed within <think> </think>
768     and <answer> </answer> tags, respectively, i.e., <think>
769     reasoning process here </think> <answer> answer here </answer>."
770   },
771   {
772     "role": "user",
773     "content": "{{Patient Information}} {{Question}}"
774   }
775 ]

```

774 Prompt used by the Preference Dataset creation process
775

```

776 You are an expert reasoning evaluator.
777 I will provide you:
778   * A question with images.
779   * The groundtruth of the question
780   * A model-generated answer, including its reasoning process.
781 Your task is to critically evaluate the reasoning based on
782 the following five aspects:
783 1. **Answer Correctness**: Is the final answer correct based
784 on the question?
785 2. **Logical Consistency**: Is the reasoning process logically
786 coherent and step-by-step valid?
787 3. **Image Analysis Involvement**: Does the reasoning process
788 demonstrate appropriate analysis of any visual information
789 mentioned or implied in the question?
790 4. **No Hallucination**: Does the reasoning process avoid
791 introducing irrelevant or hallucinated information not supported
792 by the question or known facts?
793 5. **Reflection Presence**: Does the reasoning show
794 any self-checking, verification, or reflection on
795 possible uncertainties?
796 Please return the evaluation in the following JSON format:
797   {
798     "Answer_Correctness": "Yes/No",
799     "Logical_Consistency": "Yes/No",
800     "Image_Analysis_Involvement": "Yes/No",
801     "No_Hallucination": "Yes/No",
802     "Reflection_Presence": "Yes/No"
803   }
804
805 <Question> \%s </Question>
806 <Groundtruth> \%s </Groundtruth>
807 <Answer> \%s </Answer>
808
809

```

810
811
812
813
814
815

Table 2: Performance comparison of QwenVL2.5-32B and QwenVL2.5-72B with *MedE*² across different task categories on the MedXpertQA-MM benchmark. As shown in the figure, the accuracy of each subtask improves, with the larger 72B model exhibiting a more pronounced increase compared to the 32B model.

Method	Treatment	Basic Science	Diagnosis	Reasoning	Understanding	Overall	Δ
QwenVL2.5-32B	28.13	25.78	27.61	26.07	30.87	27.40	+0.00
+Stage-I (ours)	33.03	30.31	32.19	31.60	33.21	32.05	+4.65
+Stage-II (ours)	35.93	32.57	32.86	33.54	33.39	33.50	+6.10
QwenVL2.5-72B	30.36	24.08	28.86	27.11	31.59	28.35	+0.00
+Stage-I (ours)	40.40	41.93	38.62	39.21	40.61	39.60	+11.25
+Stage-II (ours)	41.52	42.49	39.45	39.63	42.60	40.45	+12.10

822

823
824

B LLM USAGE STATEMENT

825
826
827
828
829

We used LLMs to refine the writing, including checking grammar, rephrasing, and correcting typos. To ensure the writing quality, we further check and refine the generated text. In the experimental part of this study, LLMs were employed for two specific tasks: (1) Data preparation, as described in Section 3.2, and (2) Reasoning processes judgment, detailed in Section 3.3.

830
831

C EXPERIMENTAL DETAILS

832
833
834
835
836
837
838
839

Implementation Details. All experiments are conducted on 8 NVIDIA H100 GPUs. LLaMA-Factory (Zheng et al., 2024) is used as the training framework, and vLLM (Kwon et al., 2023) serves as the backend during inference. For Stage-I, models are fine-tuned using LoRA (Hu et al., 2022) with a learning rate of 1×10^{-4} . Stage-II involves full-parameter fine-tuning with a learning rate of 1×10^{-6} , optimized using DeepSpeed (Rasley et al., 2020) with the ZeRO-3 configuration. Both stages adopt a cosine learning rate decay schedule. For models with larger parameters(i.e., 32B and 72B), we also employed LoRA in Stage-II.

840
841
842
843

D EXPERIMENTAL RESULTS WITH DIFFERENT MODEL SCALES ON MEDXPERTQA-MM

844
845
846
847

Our method demonstrates more significant performance on larger-scale models, as shown in Table 2. These findings are consistent with our observations in Section 3.2: models with more extensive prerequisite knowledge encoded within their parameter space are more capable of learning reasoning patterns from limited yet precisely structured exemplars.

848
849
850
851
852
853
854
855
856
857
858
859
860
861
862
863

864 E CASE STUDY
865

866 A 6-year-old boy presents with a forearm
867 deformity, and radiographs in Figure A confirm the
868 diagnosis. What additional diagnostic tests should
869 be performed for this patient?

870 **Correct Answer:**
871 **CBC, renal ultrasound, and echocardiogram**



872 **Response:** Alright, let's think through this case carefully. I have a 6-year-old boy who presents with a forearm deformity. The
873 radiograph confirms the diagnosis. I need to determine what additional diagnostic tests should be performed for him.
874 First, I need to identify what the diagnosis is based on the radiograph. The image shows a forearm with a single bone extending
875 from the elbow to the wrist, which appears to be a radius-like structure. There is no ulna visible. This suggests that the boy
876 has radial club hand due to congenital absence of the radius (radial aplasia). Radial club hand is a congenital anomaly
877 characterized by the absence or hypoplasia of the radius, leading to radial deviation of the wrist and hand. It's important to
878 note that this condition can be associated with other anomalies, so a thorough evaluation is necessary.
879 Now, considering potential associations, I recall that absent radius can be part of several syndromes:

1. **Thrombocytopenia-absent radius (TAR) syndrome:** Characterized by absent radii and thrombocytopenia.
2. **Fanconi anemia:** Associated with absent radii and other skeletal anomalies, as well as increased risk of malignancies.
3. **VACTERL association:** Involves vertebral defects, anal atresia, cardiac defects, tracheoesophageal fistula, renal anomalies, and limb abnormalities.
4. **Holt-Oram syndrome:** Features heart defects and upper limb anomalies.
5. **Roberts syndrome:** Includes limb defects and facial anomalies.

Given these possibilities, I need to decide which additional tests would help identify any associated conditions.

For **TAR syndrome**, I should consider ordering a complete blood count (CBC) to check for thrombocytopenia.

For **Fanconi anemia**, a CBC would also be useful since it can show pancytopenia. Additionally, a bone marrow biopsy might be needed if there's suspicion of bone marrow failure.

In **VACTERL association**, imaging studies like echocardiography (for cardiac defects), abdominal ultrasound (for renal anomalies), and possibly MRI or CT scans (for vertebral and tracheoesophageal defects) would be appropriate.

For **Holt-Oram syndrome**, cardiac evaluation is crucial, so an echocardiogram would be indicated.

Roberts syndrome typically presents with facial anomalies and limb defects, but genetic testing would be more specific for diagnosis.

Wait, am I missing anything? Could there be other tests that are more immediately relevant? Considering that hematologic abnormalities are common in some of these syndromes, starting with a CBC seems prudent. It can detect thrombocytopenia (TAR syndrome) and pancytopenia (Fanconi anemia). If the CBC reveals abnormalities, further specialized tests can be ordered. Also, given the possibility of cardiac anomalies in Holt-Oram syndrome and VACTERL association, an echocardiogram is important. Similarly, renal ultrasound is essential to rule out renal anomalies seen in VACTERL and sometimes in TAR syndrome.

Therefore, the additional diagnostic tests that should be performed for this patient are:

Order a complete blood count (CBC), Perform an echocardiogram, Conduct a renal ultrasound

880
881 Figure 8: Case illustration of models' reasoning capability in the open-ended task.
882

883 A 69-year-old woman presents with the injuries shown in Figures A and B. How should
884 this injury be classified?

885 **Answer Choices:**
886 (A) Schatzker type IV tibial plateau fracture
887 (B) Schatzker type V tibial plateau fracture
888 (C) Schatzker type VI tibial plateau fracture
889 (D) **Schatzker type III tibial plateau fracture**
890 (E) Schatzker type I tibial plateau fracture



891 **Stage-I Response:**

892 **Alright, let's take a closer look at these images.** First, I need to identify what injuries are present.
893 In Figure A, which is an X-ray image, I can see that there's a fracture on the tibial plateau. Specifically, it appears to be a fracture of the lateral
894 condyle of the tibia. There's a step-off deformity visible, indicating a significant displacement.
895 In Figure B, which is a CT scan, I can see more detail. It shows a comminuted fracture of the lateral tibial plateau with multiple fragments. The
896 fracture lines extend into the articular surface, suggesting a high-energy injury.

897 **Now, I need to recall the classification system for tibial plateau fractures proposed by Schatzker.** He divided tibial plateau fractures into six types based
898 on the location and pattern of the fracture:

- Type I: Fractures involving the anterior tibial spine.
- Type II: Fractures involving the posterior tibial spine.
- Type III: Fractures involving the medial tibial plateau.
- Type IV: Fractures involving the lateral tibial plateau.
- Type V: Fractures involving both the medial and lateral tibial plateaus.
- Type VI: Fractures involving the tibial tuberosity.

899 Given that the injury is on the lateral tibial plateau, this points me toward Type IV fractures.

900 **But wait, I should double-check to make sure I'm not missing anything.** Could this be a Type V fracture? That would involve fractures on both the medial
901 and lateral sides. However, in Type V fractures, there's usually involvement of both sides, and the fracture lines might cross the midline. In this case, the
902 fracture is confined to the lateral side. Also, could this be a Type III fracture? But Type III involves the medial tibial plateau, which isn't affected here.
903 So, Type IV seems to fit best. But I should also consider potential mistakes. For instance, if I misread the CT scan and thought there was involvement of
904 the medial side as well, I might incorrectly classify it as a Type V fracture. Another common mistake is confusing the location of the fracture. If I
905 mistakenly thought the injury was on the medial side, I'd choose Type III instead.

906 Therefore, after considering all this, I believe the correct classification is A. Schatzker type IV tibial plateau fracture.

907 **Stage-II Response:**

908 **Alright, let's tackle this problem step by step.** First, I need to carefully examine the images provided.

909 In Figure A, there's an X-ray of the knee joint. In Figure B, there's a CT scan showing the same area. Looking at Figure A, I notice that the tibial
910 plateau appears to have a significant depression or collapse. There's a noticeable gap between the tibial plateau and the femoral condyles, indicating a loss
911 of bone height. This suggests a fracture that has led to a collapse of the tibial plateau. Now, considering the CT scan in Figure B, it provides more detail.
912 It shows a large, depressed fragment on the lateral side of the tibial plateau. The fragment is displaced downward and outward, which is characteristic of
913 a lateral plateau fracture. So, putting this together, we have a lateral tibial plateau fracture with significant depression and displacement.

914 **Now, I need to recall the classification system for tibial plateau fractures proposed by Schatzker.** He divided tibial plateau fractures into six types based
915 on the location and pattern of the fracture: ...

916 Given that our patient has a lateral tibial plateau fracture with significant depression and displacement, this fits best with Schatzker Type III.

917 **Wait, but before I settle on that, I should consider whether any other options might fit better.** Option A is Schatzker Type IV, which involves the anterior and lateral portions. While there is some anterior involvement, the primary fracture line
918 seems to be lateral, making Type IV less likely.

919 Option B is Schatzker Type V, which involves the posterior and lateral portions. Again, while there's some posterior involvement, the main fracture is
920 lateral, so Type V doesn't seem to match as well.

921 Option C is Schatzker Type VI, which includes complex fractures involving multiple portions. Our patient has a single fracture line, so Type VI is
922 unlikely.

923 Option E is Schatzker Type I, which involves the anterior and medial portions. There's no medial involvement here, so Type I doesn't fit.

924 Option D is Schatzker Type III, which matches our findings perfectly.

925 So, the correct answer is D: Schatzker type III tibial plateau fracture.

926
927 Figure 9: Case illustration of the differences in the responses of models in Stage-I and Stage-II. **Blue**
928 text in the figure indicates visual hallucinations generated by the models.
929